Electronic Supplementary Material (ESI) for Materials Chemistry Frontiers.

Supporting Information

Efficient narrow green organic light-emitting diodes with low efficiency roll-offs based on iridium(III) complexes containing indolo[3,2,1-*jk*]carbazole unit

Qi-Ming Liu[1], Li Yuan[1], Xiang-Ji Liao[1], Xiao-Sheng Zhong[1], Hua-Xiu Ni[1], Yu Wang[1], Yue Zhao,[1*] and You-Xuan Zheng[1,2*]

[1]State Key Laboratory of Coordination Chemistry, Jiangsu Key Laboratory of Advanced Organic Materials, School of Chemistry and Chemical Engineering, Nanjing University, Nanjing 210093, P. R. China. E-mail: yxzheng@nju.edu.cn

[2]Shenzhen Research Institute of Nanjing University, Shenzhen 518057, P. R. China.

S1. General information

NMR measurements were conducted on a Bruker AM 400 spectrometer. High resolution electrospray mass spectra (HRMS) were measured on G6500 from Agilent for complexes. Ultraviolet-visible absorption and photoluminescence spectra were measured on a UV-3100 spectrophotometer and a Hitachi F-4600 photoluminescence spectrophotometer, respectively. Cyclic voltammetry measurements were conducted on a MPI-A multifunctional electrochemical system (Xi'an Remex Analytical Instrument Ltd. Co., China) at room temperature, with glassy carbon electrode as the working electrode, polished platinum wire electrode as the counter electrode and Ag-$AgNO_3$ (0.1 M) in CH_3CN as the reference electrode, *tetra*-n-butylammonium perchlorate (0.1 M) as the supporting electrolyte, ferrocene as the standard substance, the scan rate was 0.1 V/s. The absolute photoluminescence quantum yields (PLQYs) and the decay lifetimes (τ) of the compounds were measured with HORIBA FL-3 fluorescence spectrometer. Thermogravimetric analysis (TGA) was performed on a Pyris 1 DSC under nitrogen atmosphere at a heating rate of 10 °C min^{-1}. The single crystal of complex was carried out on a Bruker SMART CCD diffractometer using monochromated Mo Ka radiation (λ = 0.71073 Å) at room temperature. Cell parameters were retrieved using SMART software and refined using SAINT on all observed reflections.

S2. OLEDs fabrication and measurement

All OLEDs were fabricated on the pre-patterned ITO-coated glass substrate with a sheet resistance of 15 Ω sq^{-1}. The deposition rate for organic compounds is 1-2 Å s^{-1}. The phosphor and the host (2,6DCzPPy) were co-evaporated to form emitting layer from two separate sources. The cathode consisting of LiF/Al was deposited by evaporation of LiF with a deposition rate of 0.1 Å s^{-1} and then by evaporation of Al metal with a rate of 3 Å s^{-1}.

The characteristic curves of the devices were measured with a computer controlled KEITHLEY 2400 source meter with a calibrated silicon diode in air without device encapsulation. Based on the uncorrected PL and EL spectra, CIE coordinates were calculated using a test program of the Spectra scan PR650 spectrophotometer. The EQE of EL devices were calculated based on the photon energy measured by the photodiode.

S3. NMR spectra

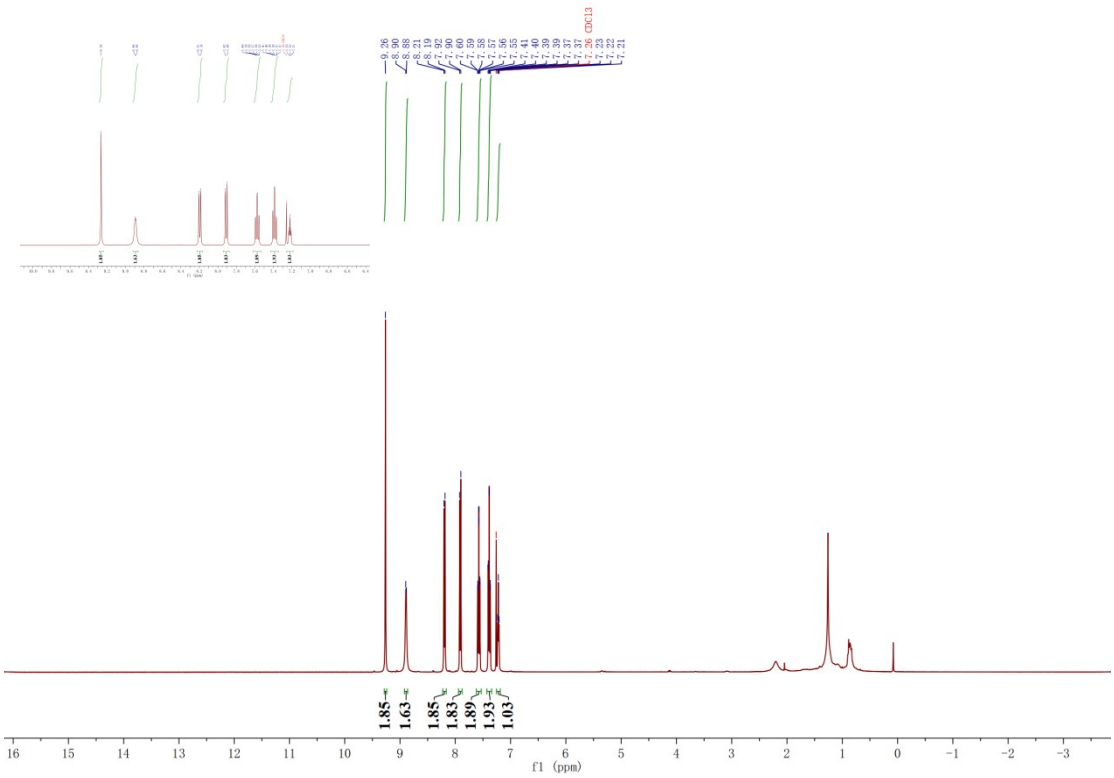

Fig. S1 ^{1}H NMR spectrum of 2-pymICz in $CDCl_3$.

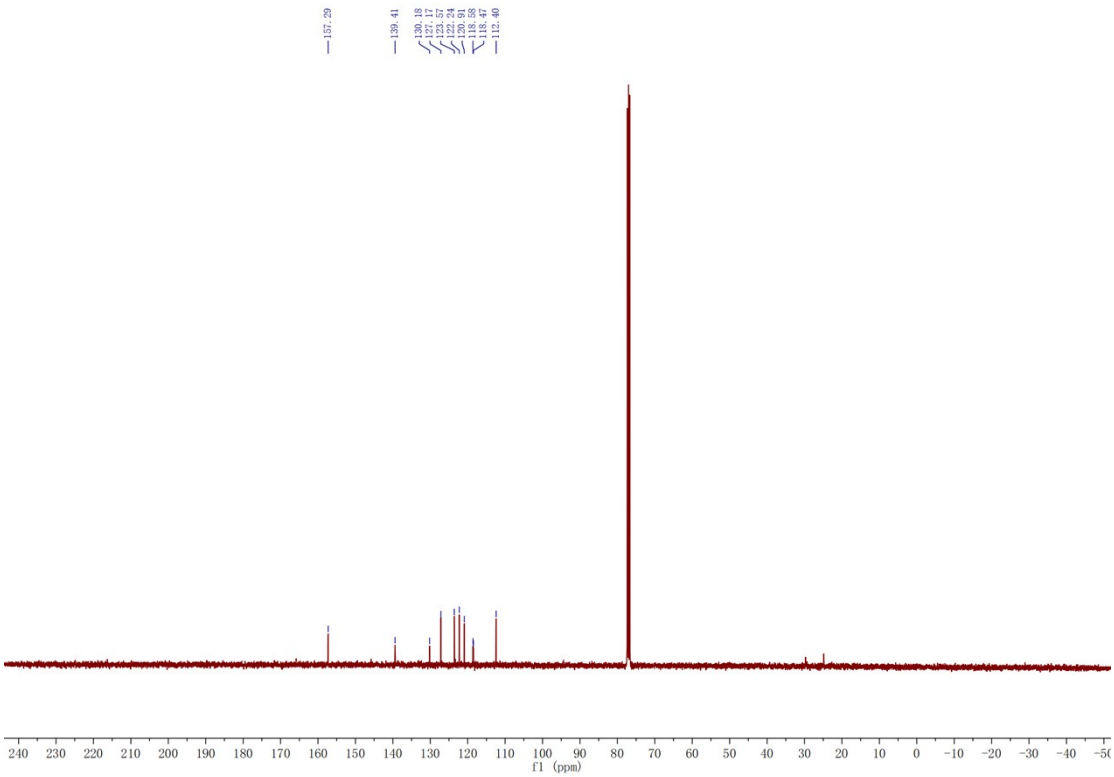

Fig. S2 ^{13}C NMR spectrum of 2-pymICz in $CDCl_3$.

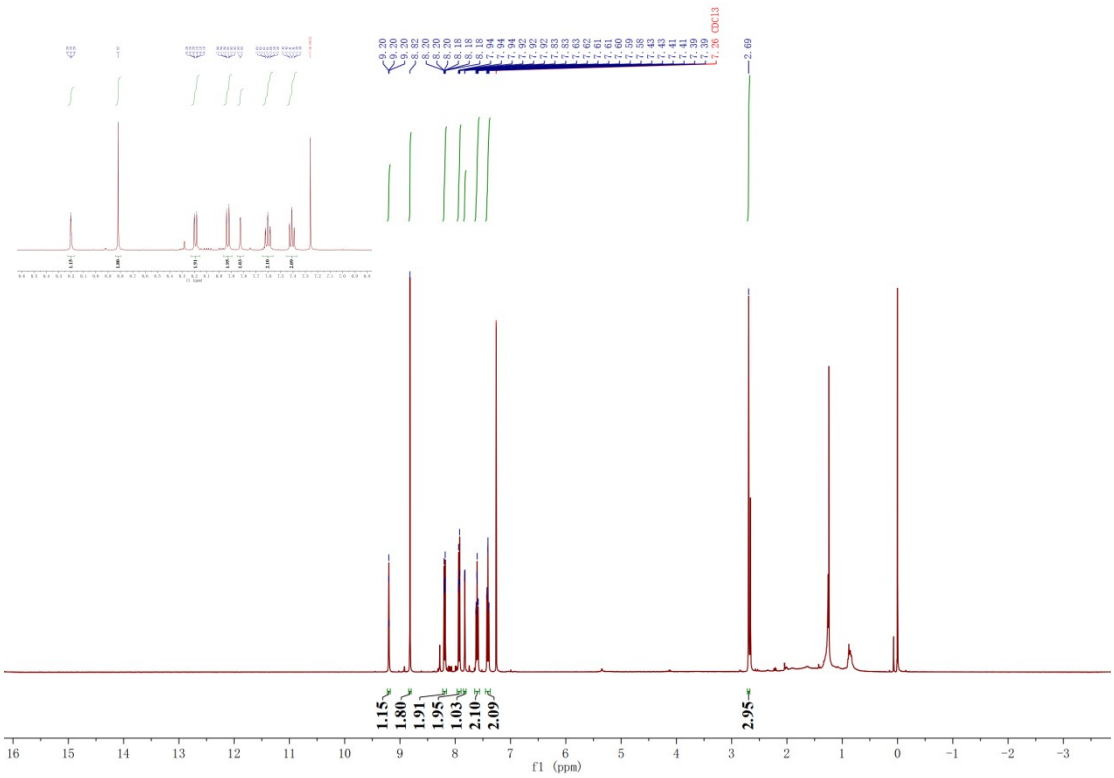

Fig. S3 ^{1}H NMR spectrum of 4-pymICz in $CDCl_3$.

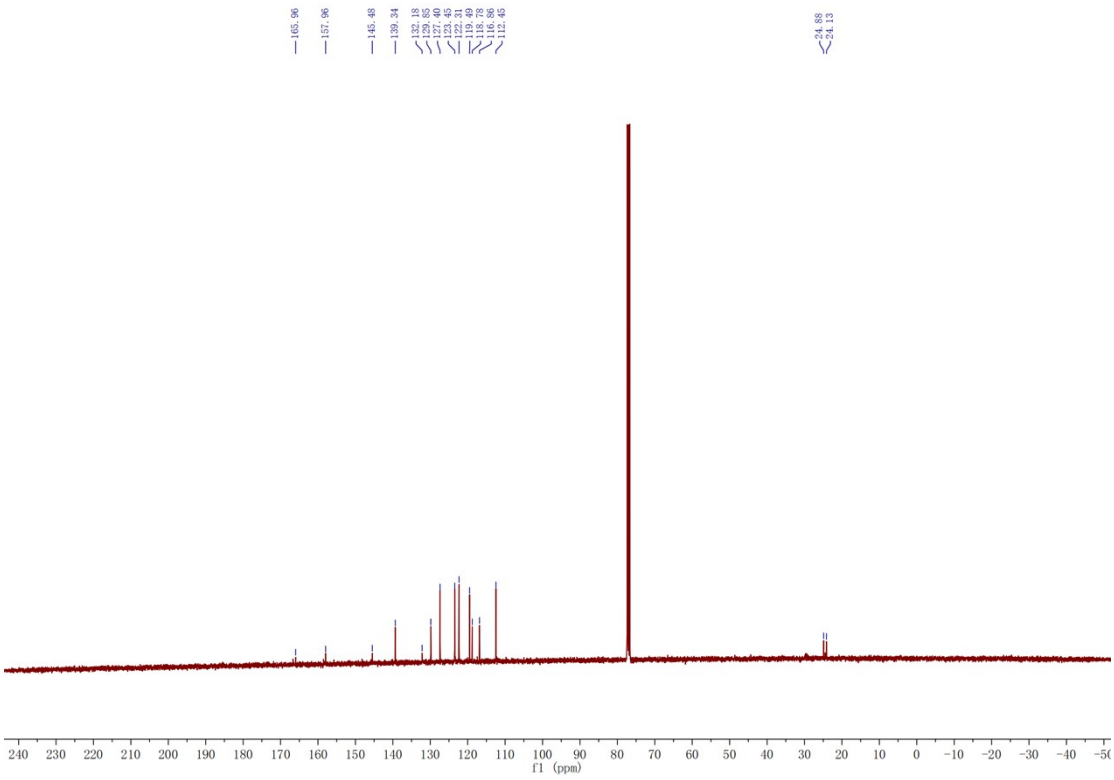

Fig. S4 ^{13}C NMR spectrum of 4-pymICz in $CDCl_3$.

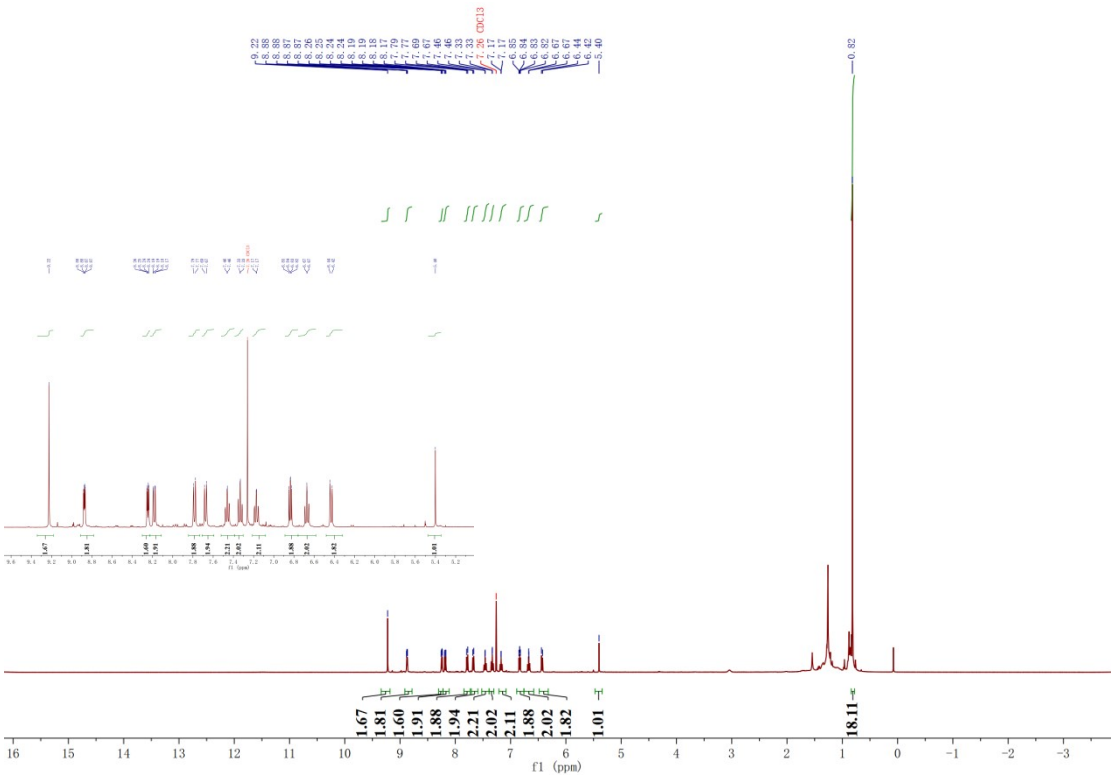

Fig. S5 ^{1}H NMR spectrum of (2-pymICz)$_2$Ir(tmd) in $CDCl_3$.

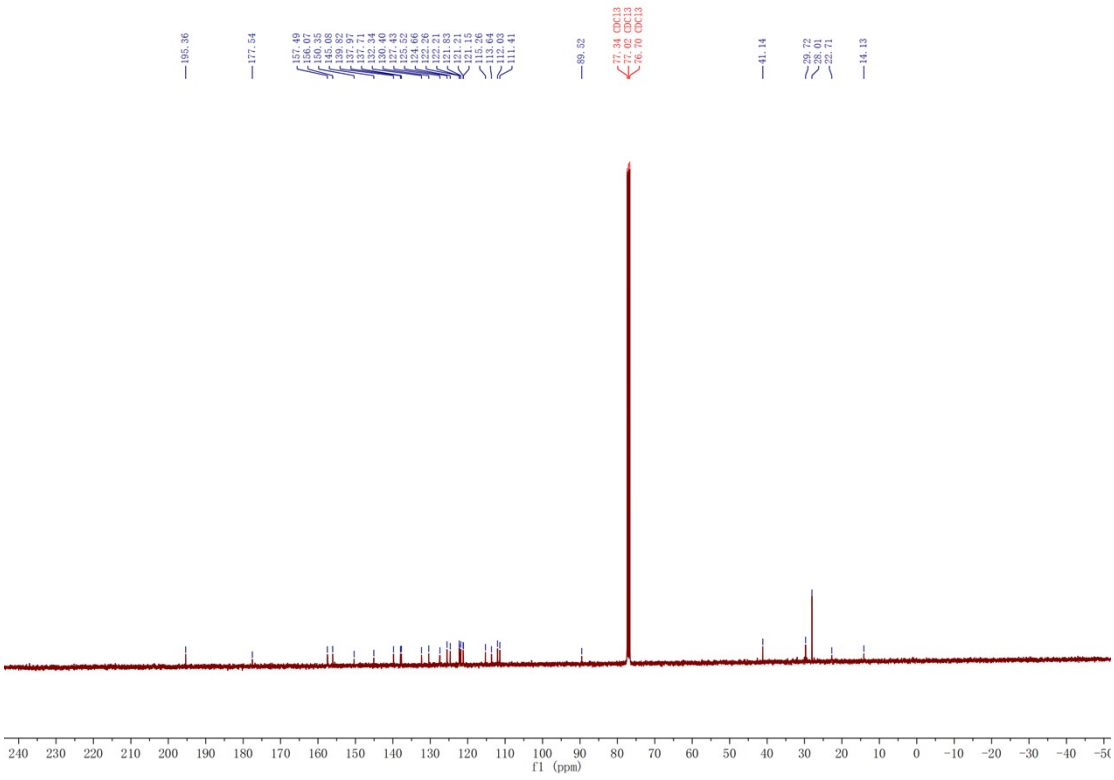

Fig. S6 ^{13}C NMR spectrum of (2-pymICz)$_2$Ir(tmd) in $CDCl_3$.

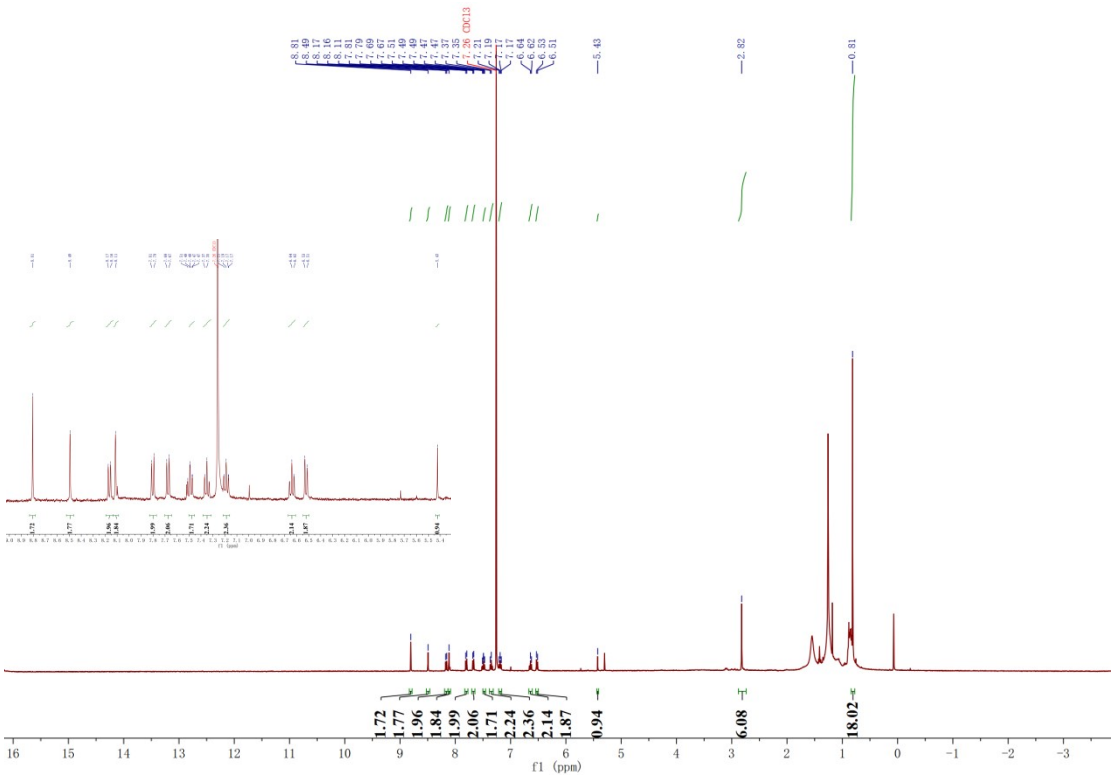

Fig. S7. ^{1}H NMR spectrum of (4-pymICz)$_2$Ir(tmd) in $CDCl_3$.

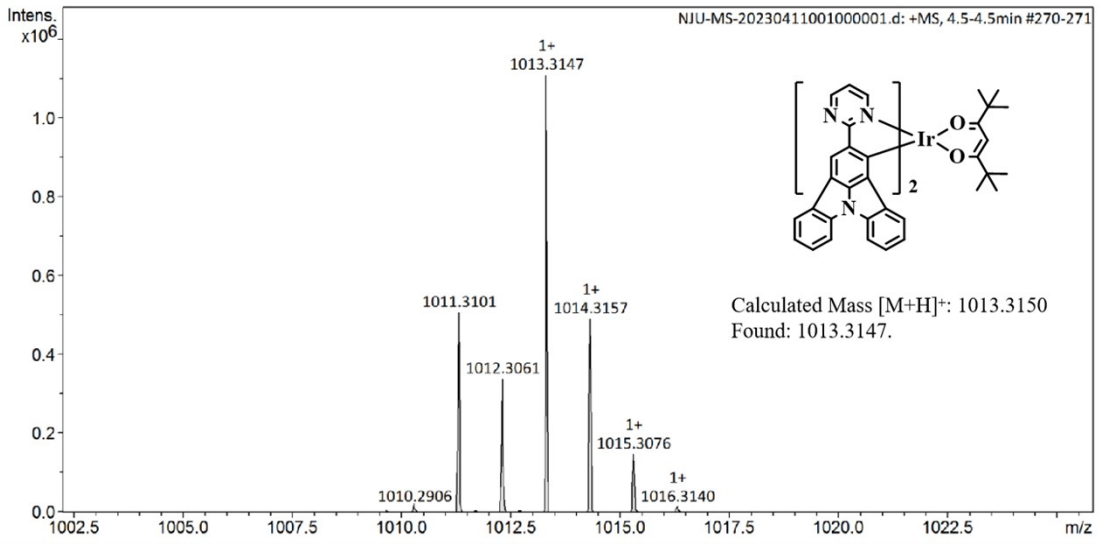

Fig. S8 HRMS spectrum of (2-pymICz)$_2$Ir(tmd).

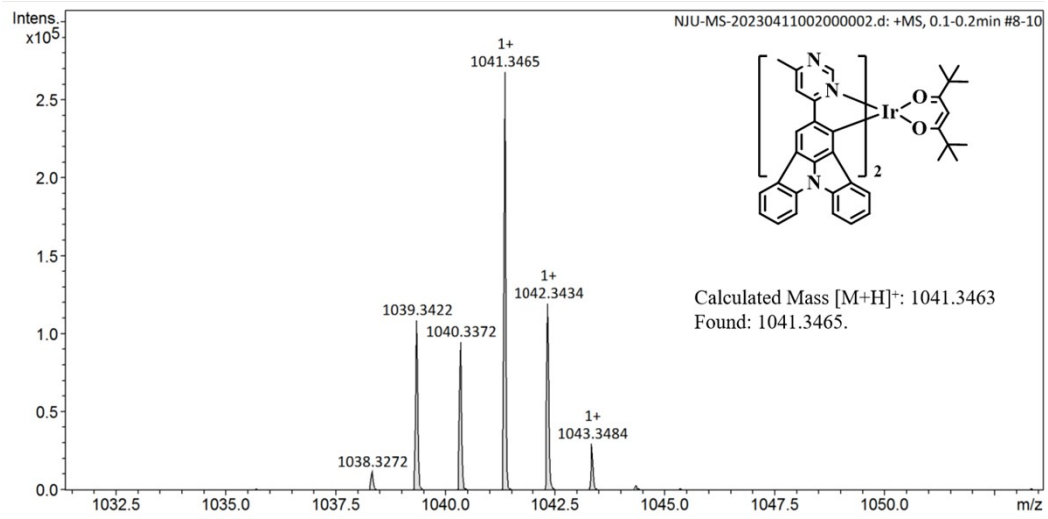

Fig. S9 HRMS spectrum of $(4\text{-pymICz})_2\text{Ir(tmd)}$.

S4. X-ray crystallographic data

Table S1. The crystallographic data of $(2\text{-pymICz})_2\text{Ir(tmd)}$.

	$(2\text{-pymICz})_2\text{Ir(tmd)}$
Formula	$C_{55}H_{43}IrN_6O_2$
Formula weight	1012.31
T (K)	193.0
Wavelength (Å)	1.34139
Crystal system	monoclinic
Space group	$P2_1/c$
a (Å)	14.6051(3)
b (Å)	12.8166(3)
c (Å)	25.1931(6)
α (deg)	90
β (deg)	99.9800(10)
γ (deg)	90
V (Å3)	4644.48(18)
Z	4
$\rho_{calculated}$ (g/cm^3)	1.569
μ (Mo Kα) (mm^{-1})	4.655
F (000)	2200.0
Range of transm factors (deg)	5.346 to 108.042
Reflns collected	38930
Unique(R_{int})	8508(0.0427)
$R_1{}^a$, $wR_2{}^b$ [I > 2s(I)]	0.0296, 0.0697
$R_1{}^a$, $wR_2{}^b$ (all data)	0.0379, 0.0742
GOF on F^2	1.039
CCDC NO	2259293

$R_1{}^a = \Sigma||F_o| - |F_c||/\Sigma|F_o|$. $wR_2{}^b = [\Sigma w(F_o{}^2 - F_c{}^2)^2/\Sigma w(F_o{}^2)]^{1/2}$

Table S2. Selected bond lengths and angles of $(2\text{-pymICz})_2\text{Ir(tmd)}$.

Selected Bonds	Bond length (Å)
Ir1-O1	2.142(2)
Ir1-O2	2.117(2)
Ir1-N1	2.021(3)
Ir1-N3	2.023(3)
Ir1-C44	1.983(3)
Ir1-C22	1.998(3)
Selected angles	(°)
O2-Ir1-O1	87.54(9)
N1-Ir1-O1	93.12(10)
N1-Ir1-O2	82.01(10)
N1-Ir1-N3	173.14(10)
N3-Ir1-O1	81.32(10)
N3-Ir1-O2	93.69(10)
C44-Ir1-O1	87.42(11)
C44-Ir1-O2	173.07(11)
C44-Ir1-N1	103.02(12)
C44-Ir1-N3	80.85(12)
C44-Ir1-C22	98.94(13)
C22-Ir1-O1	172.28(11)
C22-Ir1-O2	86.47(11)
C22-Ir1-N1	81.23(13)
C22-Ir1-N3	103.91(12)

S5. Thermal stability

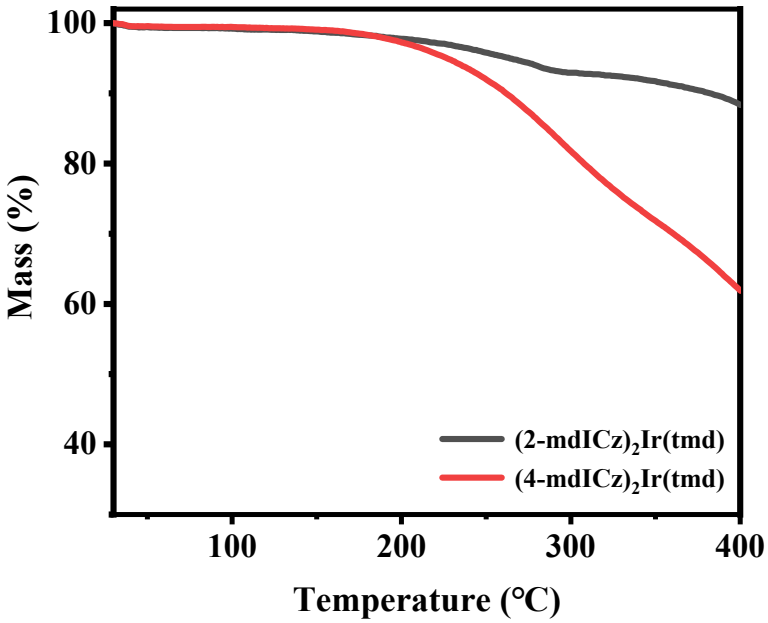

Fig. S10 TGA curves of Ir(III) complexes.

S6. Photophysical measurement

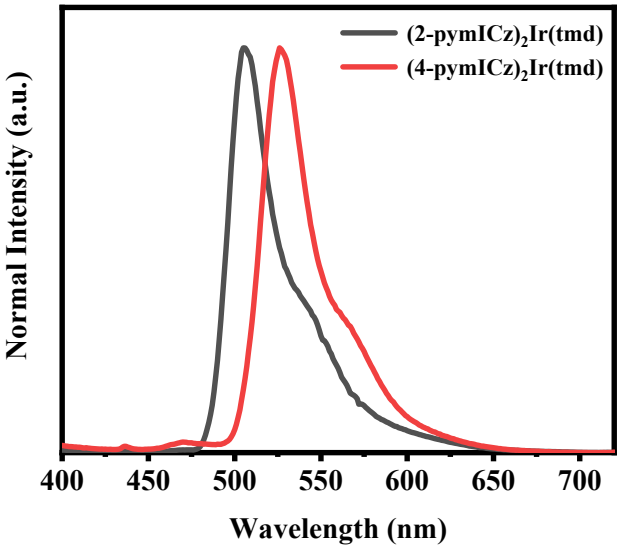

Fig. S11 PL spectra of Ir(III) complexes in DCM at 77 K.

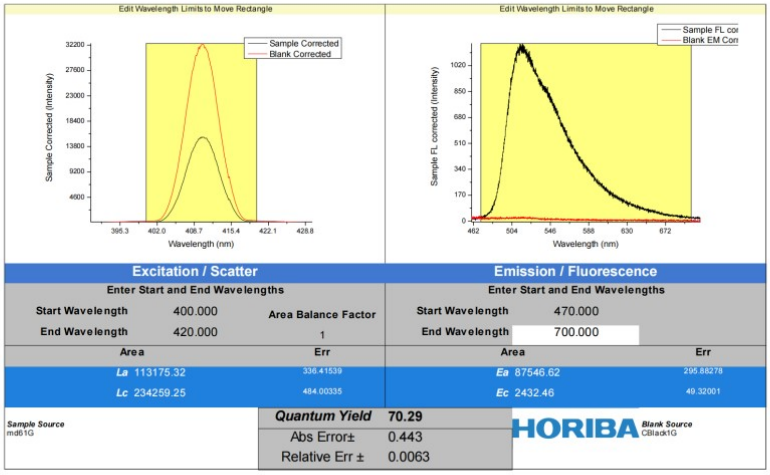

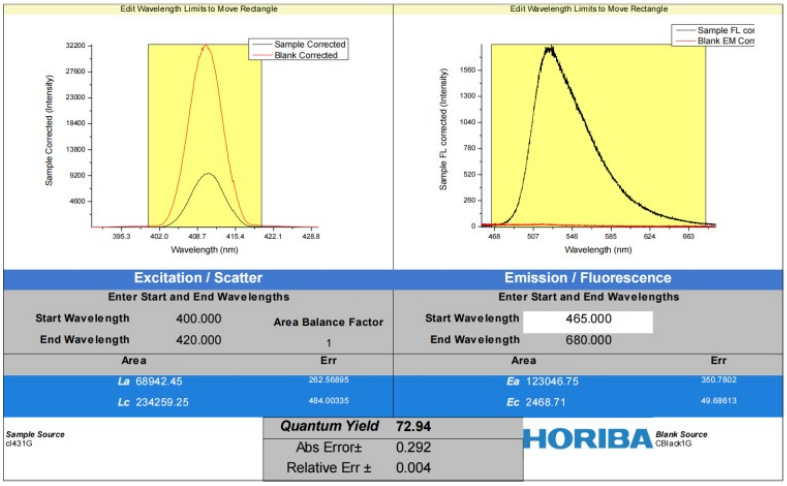

Fig. S12 PLQYs of Ir(III) complexes in deoxygenated DCM solutions (10^{-5} M).

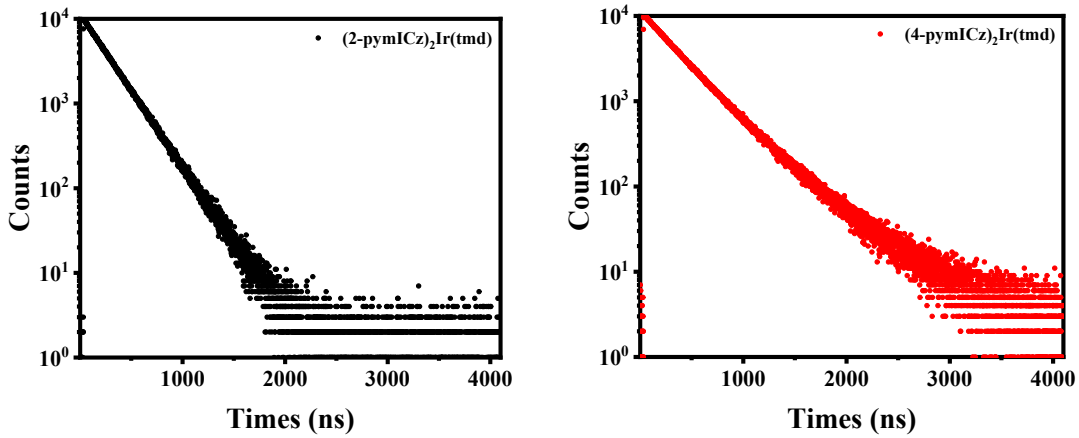

Fig. S13 Phosphorescence lifetime curves of Ir(III) complexes in deoxygenated DCM solutions (10^{-5} M).

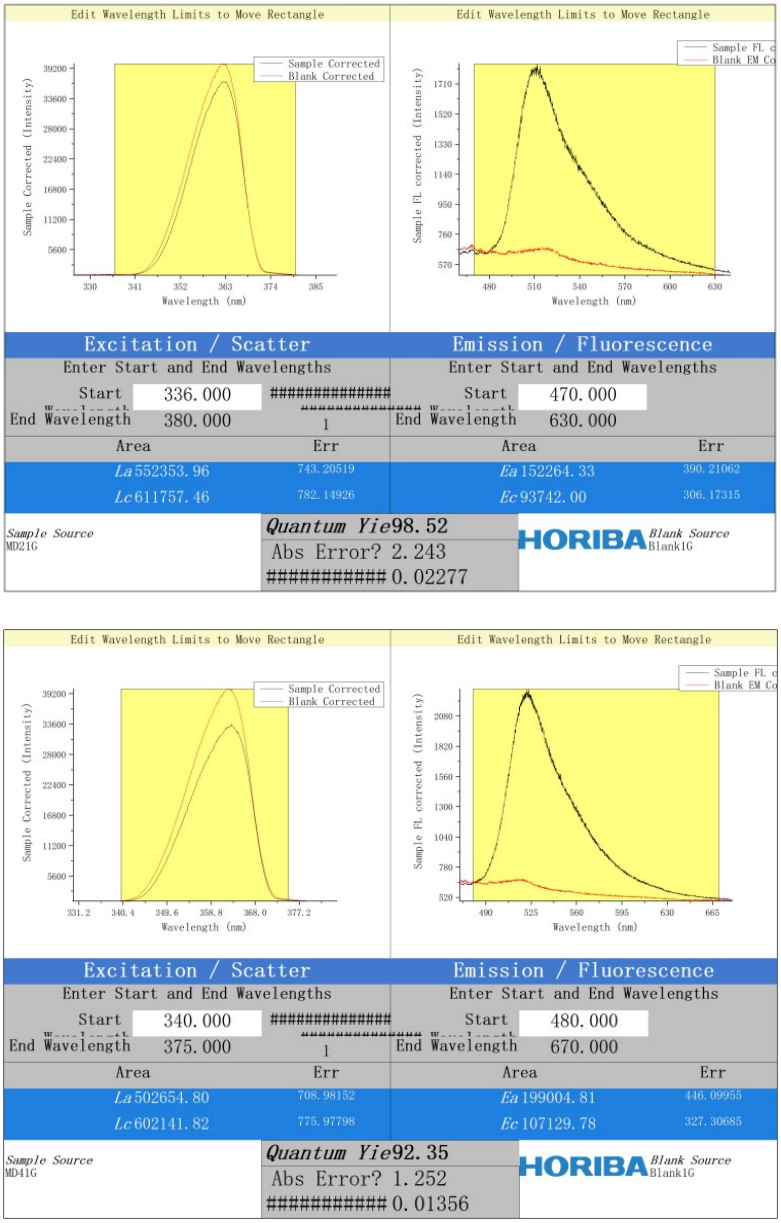

Fig. S14 PLQYs of Ir(III) complexes in doped films (7 wt% in 2,6DCzPPy).

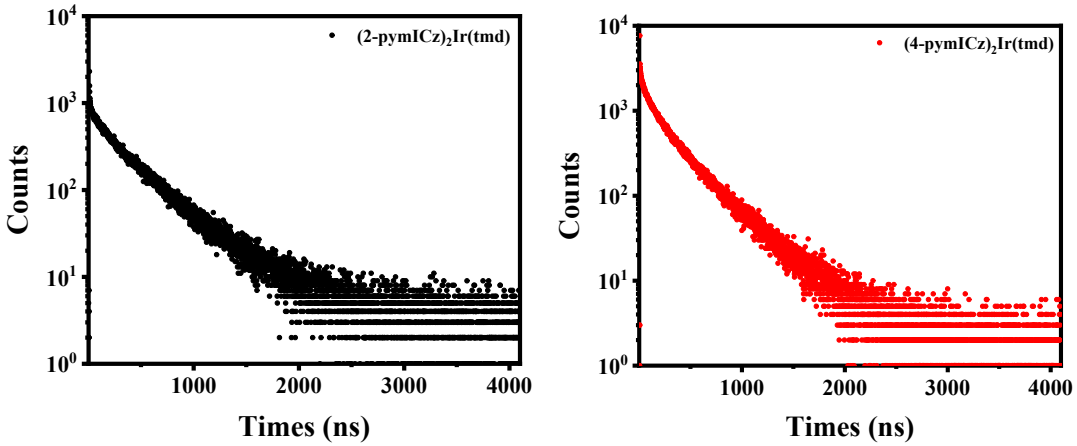

Fig. S15 Phosphorescence lifetime curves of Ir(III) complexes in doped films (7 wt% in 2,6DCzPPy).

S7. Electrochemical measurement

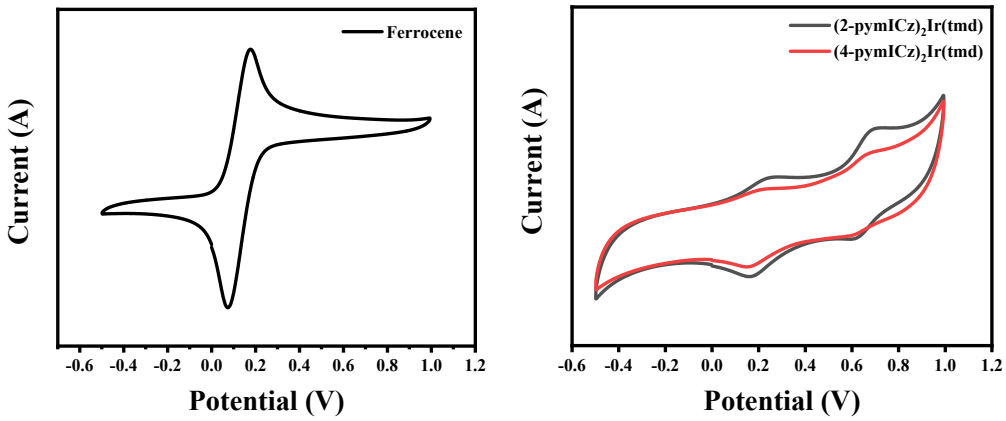

Fig. S16 CV curves of Fc and two Ir(III) complexes in deoxygenated CH_3CN solutions (10^{-5} M).

S8. Theoretical calculations

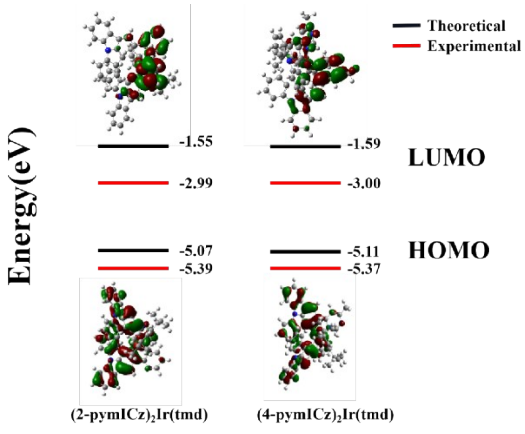

Molecular structure	Fragments' Composition			
(2-pymICz)2Ir(tmd)		Iridium	Main Ligand	Ancillary Ligand
	HOMO	24.90%	72.12%	2.98%
	LUMO	5.32%	93.16%	1.52%
(4-pymICz)2Ir(tmd)		Iridium	Main Ligand	Ancillary Ligand
	HOMO	28.09%	67.53%	4.38%
	LUMO	3.42%	95.32%	1.26%

Fig. 17 Electron cloud distributions, HOMO/LUMO diagrams, and composition of each fragment of Ir(III) complexes obtained from theoretical calculations, cyclic voltammetry curves and UV-Vis spectra.

Table S3. TD-DFT calculations with IFCT method of $(2\text{-pymICz})_2\text{Ir(tmd)}$.

Donor	Acceptor		
	Iridium	Ancillary ligand	Main ligand
Iridium	0.013	0.002	0.255
Ancillary ligand	0.001	0.000	0.026
Main ligand	0.035	0.006	0.660

Table S4. TD-DFT calculations with IFCT method of $(4\text{-pymICz})_2\text{Ir(tmd)}$.

Donor	Acceptor		
	Iridium	Ancillary ligand	Main ligand
Iridium	0.009	0.002	0.287
Ancillary ligand	0.001	0.000	0.035
Main ligand	0.020	0.004	0.641

S9. Electroluminescence measurement

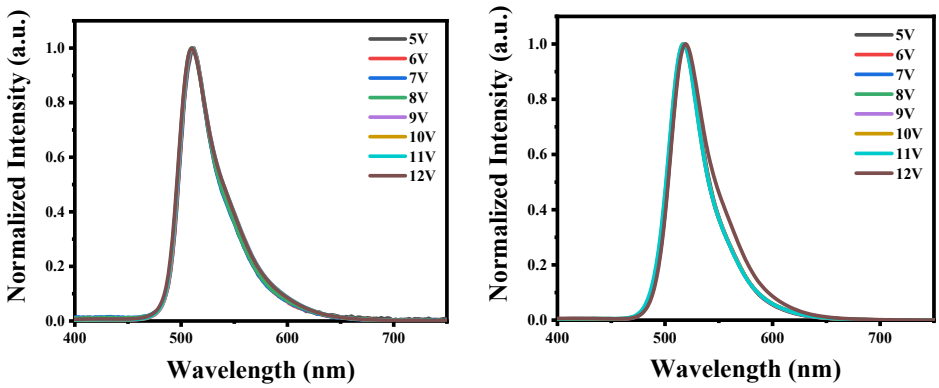

Fig. S18 EL spectra of D1 and D2 taken at different voltages from 5 to 12 V.